

**Title:** New insights into the evolution of glutamine synthetase isoenzymes in plants

**Authors:** José Miguel Valderrama-Martín<sup>1,3</sup>, Francisco Ortigosa<sup>1</sup>, Concepción Ávila<sup>1</sup>, Francisco M. Cánovas<sup>1</sup>, Bertrand Hirel<sup>2</sup>, Francisco R. Cantón<sup>3\*</sup>, Rafael A. Cañas<sup>3\*</sup>.

**Addresses:** <sup>1</sup>Grupo de Biología Molecular y Biotecnología, Departamento de Biología Molecular y Bioquímica, Universidad de Málaga, Campus Universitario de Teatinos, 29071-Málaga, Spain.

<sup>2</sup>Institut National de Recherche pour l'Agriculture, l'Alimentation et l'Environnement (INRAE), Centre de Versailles-Grignon, RD 10, 78026 Versailles cedex, France.

<sup>3</sup>Integrative Molecular Biology Lab, Universidad de Málaga, Campus Universitario de Teatinos, 29071-Málaga, Spain.

**Correspondence:** \*Francisco R. Cantón, Departamento de Biología Molecular y Bioquímica, Facultad de Ciencias, Universidad de Málaga, Campus Universitario de Teatinos s/n, E-29071 Málaga, Spain. E-mail: [frcanton@uma.es](mailto:frcanton@uma.es) Phone number: +34-951-953220 Fax number: +34-952-132041.

\*Rafael A. Cañas, Departamento de Biología Molecular y Bioquímica, Facultad de Ciencias, Universidad de Málaga, Campus Universitario de Teatinos s/n, E-29071 Málaga, Spain. E-mail: [rcanas@uma.es](mailto:rcanas@uma.es) Phone number: +34-925-134272 Fax number: +34-952-132041.

**Authors E-mails:** José Miguel Valderrama-Martín ([jmvalderrama@uma.es](mailto:jmvalderrama@uma.es)); Francisco Ortigosa ([fortigosa@uma.es](mailto:fortigosa@uma.es)); Concepción Ávila ([cavila@uma.es](mailto:cavila@uma.es)); Francisco M. Cánovas ([canovas@uma.es](mailto:canovas@uma.es)); Bertrand Hirel ([bertrand.hirel@inrae.fr](mailto:bertrand.hirel@inrae.fr)); Francisco R. Cantón ([frcanton@uma.es](mailto:frcanton@uma.es)); Rafael A. Cañas ([rcanas@uma.es](mailto:rcanas@uma.es)).

**ORCID IDs:** JMVM (0000-0003-1350-899X); FO (0000-0002-7517-7594); CA (0000-0001-8817-7529); FMC (0000-0002-4914-2558); BH (0000-0002-5518-3671); FRC (0000-0001-6917-8630) and RAC (0000-0001-9727-5585)

**Keywords:** Glutamine synthetase, phylogeny, plant evolution, nitrogen metabolism, new gene classification

## 1 **ABSTRACT**

2 Glutamine synthetase (GS) is a key enzyme responsible for the incorporation of inorganic nitrogen  
3 in the form of ammonium into the amino acid glutamine. The genes encoding GS are among the  
4 oldest existing genes in living organisms. In plants, two groups of functional GS enzymes are  
5 found: eubacterial *GSIIb* (*GLN2*) and eukaryotic *GSIIe* (*GLN1/GS*). Phylogenetic analyses have  
6 shown that the *GLN2* group originated from bacteria following horizontal gene transfer. Only  
7 *GLN1/GS* genes are found in vascular plants, which suggests that they are involved in the final  
8 adaptation of plants to terrestrial life. The present phylogenetic study reclassifies the different GS of  
9 seed plants into three clusters: *GS1a*, *GS1b* and *GS2*. The presence of genes encoding *GS2* has been  
10 expanded to Cycadopsida gymnosperms, which suggests the origin of this gene in a common  
11 ancestor of Cycadopsida, Ginkgoopsida and angiosperms. *GS1a* genes have been identified in all  
12 gymnosperms, basal angiosperms and some Magnoliidae species. Previous studies in conifers and  
13 the gene expression profiles obtained in ginkgo and magnolia in the present work could explain the  
14 absence of *GS1a* in more recent angiosperm species (e.g., monocots and eudicots) due to the  
15 redundant roles of *GS1a* and *GS2* in photosynthetic cells. Altogether, the results provide a better  
16 understanding of the evolution of plant GS isoenzymes and their physiological roles, which is  
17 valuable for improving crop nitrogen use efficiency and productivity.

18

## 19 **INTRODUCTION**

20 Glutamine synthetase (GS, EC 6.3.1.2) catalyzes the incorporation of ammonium into glutamate  
21 using ATP to produce glutamine while releasing Pi and ADP (Heldt and Piechulla, 2011). GS is an  
22 enzyme of major importance, as it represents the main, if not the only, mechanism incorporating  
23 inorganic nitrogen (N) into organic molecules in virtually all living organisms (Shatters et al. 1989).  
24 It has been suggested that the genes encoding GS are not only one of the oldest genes in the  
25 evolutionary history (Kumada et al. 1993) but also represent an excellent “molecular clock”, which  
26 can be used to perform phylogenetic studies (Pesole et al. 1991).

27 Three GS superfamilies have been identified, namely, GSI, GSII and GSIII, with the corresponding  
28 proteins characterized by different molecular masses, different numbers of subunits and their  
29 occurrence in the three different domains of life (*Bacteria*, *Archaea* and *Eukarya*) (Ghoshroy et al.  
30 2010). The GSI superfamily was first found in prokaryotes, although its presence in mammals and  
31 plants has also been reported (Mathis et al. 2000; Nogueira et al. 2005; Kumar et al. 2017). The  
32 GSII superfamily was described as a group characteristic of *Eukarya* and some *Bacteria* such as  
33 *Proteobacteria* and *Actinobacteria* (James et al. 2018). However, the nucleotide sequences  
34 deposited in public databases indicate that this GS superfamily is also present in *Euryarchaeota*, a

35 phylum of the *Archaea* domain. Finally, the GSIII superfamily is characteristic of bacteria,  
36 including cyanobacteria (James et al. 2018), and some eukaryotes, such as diatoms and other  
37 heterokonts, suggesting that GSIII is present in the nucleus of early eukaryotes (Robertson et al.  
38 2006). In a number of studies, the hypothesis that these three gene superfamilies appeared prior to  
39 the divergence of eukaryotes and prokaryotes has been proposed (Robertson et al. 2006).

40 In plants, glutamine synthesis is catalyzed by enzymatic proteins belonging to the GSII superfamily.  
41 Two main groups of GSII have been shown to occur in the Viridiplantae group, one of eukaryotic  
42 origin, GSII (GSIIe), and the other of eubacterial origin, GSII (GSIIb). *GSIIb* genes are the result of  
43 horizontal gene transfer (HGT) following the divergence of prokaryotes and eukaryotes, which in  
44 turn represent a sister group of  $\gamma$ -proteobacteria *GSII* (Tateno et al. 1994, Ghoshroy et al. 2010).  
45 Since N is one of the main limiting nutrients for plant growth and development, the functions and  
46 characteristics of GS have been extensively studied in a large number of vascular plant species, and  
47 particularly in crops (Plett et al. 2017; Mondal et al. 2021). It is generally indicated that  
48 angiosperms contain two groups of nuclear genes encoding GSIIe represented by cytosolic GS  
49 (GS1) and plastidic GS (GS2), each playing distinct physiological roles (Ghoshroy et al. 2010; Hirel  
50 and Krapp 2021). GS2 is generally encoded by a single gene, whereas GS1 is encoded by a small  
51 multigene family (Cánovas et al. 2007; James et al. 2018). Phylogenetic analyses suggest that *GS2*  
52 probably evolved from *GS1* gene duplication (Biesiadka and Legocki 1997) that diverged from a  
53 common ancestor 300 million years ago (mya). Therefore, this gene duplication probably occurred  
54 before the divergence of monocotyledons and dicotyledons (Bernard and Habash 2009).  
55 Interestingly, the gene encoding GS2 is present in the gymnosperm *Ginkgo biloba* (García-  
56 Gutiérrez et al. 1998; Guan et al. 2016). This gene is absent in all the other gymnosperms examined  
57 thus far, including conifers (Coniferopsida) and gnetales (Gnetopsida), in which the gene encoding  
58 GS2 has not been found in their genomes (Birol et al. 2013; Nystedt et al. 2013; Neale et al. 2014;  
59 Zimin et al. 2014; Stevens et al. 2016; Neale et al. 2017; Wan et al. 2018; Kuzmin et al. 2019;  
60 Mosca et al. 2019; Scott et al. 2020). Furthermore, it seems to also be absent in cycas  
61 (Cycadopsida), since the GS2 protein was not detected in western blot analyses (Miyazawa et al.  
62 2018).

63 In both angiosperm and gymnosperm plants, the synthesis and relative activity of the different GS  
64 isoforms are regulated in a species-specific manner but also according to a plant's developmental  
65 stage, tissue, N nutritional status, and to the environmental conditions (Cánovas et al. 2007; Bernard  
66 and Habash 2009, Mondale et al. 2021). Consequently, each GS isoform plays a different role  
67 during N assimilation and N remobilization throughout a plant's life cycle (Thomsen et al. 2014;  
68 Hirel and Krapp 2021). GS2 predominates in photosynthetic tissues such as leaf mesophyll cells in

69 order to assimilate the ammonium generated from nitrate reduction and released during  
70 photorespiration (Wallsgrave et al. 1987; Blackwell et al. 1987; Tegeder and Masclaux-Daubresse  
71 2017). In contrast, GS1 is present in almost all plant organs and tissues (Lea and Mifflin 2018).  
72 Cytosolic GS isoforms are mostly involved in primary N assimilation in roots and N remobilization  
73 and translocation in shoots (Thomsen et al. 2014). As such, it has been shown that they play a key  
74 role during plant growth and development, notably for biomass and storage organ production (Xu et  
75 al. 2012; Krapp 2015; Havé et al. 2017; Amieur et al. 2021). In conifers, due to the absence of GS2,  
76 studies have focused on GS1a and GS1b, which are each encoded by a single gene. These two  
77 cytosolic isoforms of GS also exhibit distinct molecular and kinetic properties (Ávila-Sáez et al.  
78 2000; de la Torre et al. 2002). GS1a has been proposed to fulfill the same function as GS2 in  
79 angiosperms due to its close relationship with chloroplast development and to the presence of  
80 ammonium arising from photorespiration. This hypothesis was also supported by the fact that the  
81 gene encoding GS1a is expressed in photosynthetic organs, notably in chlorophyllous parenchyma  
82 cells (Ávila et al. 2001), and that its expression is also upregulated in the presence of light (Cantón  
83 et al. 1999; Gómez-Maldonado et al. 2004). Moreover, GS1b is phylogenetically and functionally  
84 more related to the cytosolic isoforms of GS in angiosperms than to those of GS1a in conifers  
85 (Ávila-Sáez et al. 2000; Cánovas et al. 2007).

86 In this work, the increasing number of plant genome sequences made available in public databases  
87 were gathered to perform a deep phylogenetic analysis of the GSII family. The present study  
88 includes representative GS sequences from the entire plant evolutionary spectra, including those  
89 from monocot and dicot angiosperms and a number of model species that were representative of  
90 other taxa. This new phylogenetic study allowed us to propose a revised classification and  
91 nomenclature for the different GS isoforms in seed plants. In addition, GS gene expression  
92 experiments were conducted in *G. biloba*, *Magnolia grandiflora* and *Pinus pinaster* in order to  
93 strengthen the results obtained in the GS1a phylogeny.

94

## 95 **RESULTS**

96 A total of 168 nucleotide sequences from coding regions (CDS) and the corresponding protein  
97 sequences of the genes encoding GSII from 45 different Viridiplantae species were retrieved from  
98 different public databases or assembled using next-generation sequencing (NGS) data from the  
99 Sequence Read Archive (SRA) database (Table S1). Additionally, *Escherichia coli glnA* (GSI) was  
100 used as an external group. The sequences and species analyzed cover the evolutionary history of  
101 Viridiplantae and included members of the main Viridiplantae clades unless the sequences were not  
102 available in the public databases. These sequences were used to perform phylogenetic analyses to

103 assess GSII evolution in Viridiplantae. The final names of the sequences were assigned depending  
104 on phylogenetic analyses (Figures 1 and 2, Table S1). The GSIIb sequences were named GLN2  
105 following the nomenclature of GLN2, the gene encoding GS in *Chlamydomonas reinhardtii*. The  
106 GSIIe group, which corresponds to species older than the Embryophyta, was named GLN1. The  
107 sequences from Embryophyta species were named GS1, except those included in the group of the  
108 Spermatophyta GS2 sequences.

109 The phylogenetic studies were conducted with nucleotide sequences using Bayesian analyses  
110 (Figures 1 and S1). For the protein sequences, a maximum likelihood approach was used (Figures 2  
111 and S2). The results were similar for the main GS groups whether the nucleotide or the protein  
112 sequences were analyzed. The *KnGLNA* sequence of *Klebsormidium nitens*, a charophyte green  
113 algae, was the most divergent GS close to the outer sequence *EcGLNA* (GSI) of *E. coli* (Figures S1  
114 and S2). Both sequences were very distant from the other plant GS genes (mean length 2.0756),  
115 with a node/branch probability of 1 in the Bayesian analysis.

116 The first cluster contained all GLN2 (GSIIb) sequences. Notably, no GLN2 sequence was identified  
117 in vascular plants (Tracheophyta). In the protein sequence analyses, we observed that the GLN2  
118 cluster shared a common origin. In addition, different subgroups for GLN2 were identified in the  
119 nucleotide sequence clustering analyses. These GLN2 subgroups were distant from the other plant  
120 GS sequences (GSIIe; mean length 0.7142) (Figures S1 and S2). For both the GLN2 nucleotide and  
121 protein sequences, the node/branch probability/bootstrap was high (>0.65). In all GLN2 sequences,  
122 we found a predicted localization in the chloroplast when using the TargetP software except for  
123 UpGLN2, ChrGLN2.1 and ChrGLN2.2 for which we found mitochondrial localization (Figures 1  
124 and 2, Table S1).

125 The most ancient GSIIe plant sequences were named GLN1, and in both analyses, they were  
126 distributed in a main group containing four nonclustered sequences, including *KnGLN1*  
127 (*Klebsormidiophyceae* class), *CgGLN1.1* and *CgGLN1.2* (*Coleochaetophyceae* class) and *PmGLN1*  
128 (*Zygnemophyceae* class). These four sequences were in an intermediary position between the main  
129 GLN1 cluster and the other GS sequences from land plants. A predicted chloroplast localization  
130 was only found for *CgGLN1.2* (Figures 1 and 2).

131 Three clusters were identified in seed plants (Spermatophyta), including plastidic GS2 and  
132 gymnosperm GS1a-like and GS1b-like sequences (Figures 1 and 2). Interestingly, within the GS2  
133 group, three sequences from gymnosperms were identified (*GbGS2*, *ChaGS2* and *EnGS2*). They  
134 corresponded to a ginkgo and two Cycadopsida sequences. The GS1a-like group contained known  
135 GS1a sequences from gymnosperms and GS1 from basal angiosperms and from some Magnoliidae  
136 except Ranunculales, Proteales, Liliopsida and Eudycotyledon species. However, an ortholog of the

137 *GS1a* gene was not identified in the genome of *Piper nigrum*, a Magnoliidae species from the  
138 Piperales order (Hu et al. 2019). Finally, the GS1b-like cluster contained GS1b found in  
139 gymnosperms and the GS1 enzymes previously characterized in angiosperms.

140 The phylogeny of GS from Anthocerotophyta, Marchantiophyta, Bryophyta, Lycopodiopsida and  
141 Polypodiopsida was more complex than that of Spermatophyta, especially when the protein  
142 sequences were analyzed (Figures 1 and 2). However, with the cognate gene sequences,  
143 Anthocerotophyta, Marchantiophyta, Bryophyta, and Lycopodiopsida were in a basal position  
144 compared to the other Embryophyta species. Such a distribution corresponded to the expected  
145 evolutionary relationships between plant species, except for the outlier sequence *MpGS1.4* that was  
146 found in the GS1a-like cluster (Figure 1). Fern (Polypodiopsida) GS genes were grouped into two  
147 clusters. The first one contained most of the nucleotide sequences linked to the GS1a-like  
148 sequences, and the second one was grouped with GS2 and was composed of *EdGS1.4*, *OvGS1.2*,  
149 *OvGS1.3*, *VsGS1.1*, *LjGS1.1*, *AzfGS1.5*, *AspGS1.5*, *PglyGS1.1* and *PglyGS1.4*. For these two  
150 clusters, the mean probabilities were very high (0.9 and 0.97, respectively) when Bayesian analysis  
151 was used (Figure 1, Figure S1).

152 In contrast, the phylogenetic relationships with the protein sequences were unclear because of a  
153 different cluster distribution and the occurrence of outlier sequences such as *PglyGS1.3* and  
154 *MpGS1.4* (Figure 2). Most of the Marchantiophyta and Bryophyta GS enzymes were grouped with  
155 most of the Polypodiopsida sequences, although *MpGS1.3* and *AnaGS1* clustered with the GS2  
156 from Spermatophyta. This group of GS proteins was closer to that of the Spermatophyta GS1  
157 compared to GS2, even though the node/branch bootstraps were very low (<1). The Lycopodiopsida  
158 GS enzymes were grouped together with GS1b-like protein sequences even though the node/branch  
159 bootstrap was also very low (<1). Nevertheless, two sequences (*SmGS1.3* and *SmGS1.4*) were  
160 grouped with the Spermatophyta GS1a cluster together with four Polypodiopsida sequences  
161 (*EdGS1.4*, *OvGS1.2*, *OvGS1.3* and *VsGS1.2*) (Figure 2).

162 As expected, for all GS2, the presence of a signal peptide which allows the targeting of the protein  
163 to the chloroplast was predicted (Figures 1 and 2, Table S1). Only five of the remaining  
164 Embryophyta proteins were predicted to be localized in the chloroplast, including *IsGS1.2* and  
165 *PdGS1.2* from Lycopodiopsida species and *EdGS1.2*, *EdGS1.3* and *AfGS1.2* from Polypodiopsida  
166 species. Moreover, one could observe that these five GS enzymes did not belong to the GS2 cluster  
167 (Figures 1 and 2, Table S1).

168

169 **Spermatophyta GS gene expression**

170 To further decipher the role of GS1a in ginkgo and in angiosperms, the level of expression of  
171 different GS genes was quantified in *P. pinaster*, *G. biloba* and *M. grandiflora*. Maritime pine (*P.*  
172 *pinaster*) was included in the study because the role and gene expression pattern of GS1a is well  
173 established in this gymnosperm, characterized by the absence of a gene encoding GS2 (Cánovas et  
174 al. 2007). The gymnosperm *G. biloba* and the angiosperm *M. grandiflora* were also studied because  
175 they possess GS genes corresponding to the three main Spermatophyta GS groups (GS1a, GS1b and  
176 GS2).

177 In maritime pine seedlings, the profiles of *PpGS1a* and *PpGS1b* gene expression were analyzed  
178 under different light/dark regimes (Figure 3): germination with a light/dark (L/D) cycle (16 hours of  
179 light and 8 hours of darkness), continuous darkness, and two opposite nycthemeral regimes (from  
180 light to dark and from dark to light). *PpGS1a* was mainly expressed in the needles irrespective of  
181 the light/dark regime and in the stem only during the L/D cycle. In roots, the *PpGS1a* expression  
182 level was at the limit of detection under the four different light/dark conditions. In the needles,  
183 *PpGS1a* reached the highest level of expression in the dark-light transition, even though it was  
184 slightly lower under the L/D cycle. Compared to these two conditions, the *PpGS1a* expression level  
185 in the needles was at least five times lower when the plants were placed under continuous darkness  
186 and approximately twice lower following a light-dark transition. In contrast, *PpGS1b* was expressed  
187 in all three organs. In the needles and in the roots, its expression level was significantly higher only  
188 during the light-dark transition. In the stem, the *PpGS1b* expression level was the highest when the  
189 seedlings were grown under the L/D cycle.

190 In *G. biloba* seedlings, *GbGS1a*, *GbGS2* and *GbGS1b* (1 to 3) expression levels were quantified  
191 during the L/D cycle and when plants were placed under continuous darkness (Figure 4A). The  
192 absence of leaves in *G. biloba* seedlings germinated under continuous darkness did not allow us to  
193 quantify the level of GS gene expression in this organ (García-Gutiérrez et al. 1998). Therefore,  
194 light/dark transition experiments were carried out using the leaves of one-year-old *G. biloba* plants  
195 (Figure 4B). The amount of *GbGS2* transcripts was very low both in the stems and roots when the  
196 seedlings were grown under L/D or continuous darkness conditions. In contrast, under these two  
197 conditions, the *GbGS2* expression level was at least 20-fold higher in the leaves. Although the  
198 amount of *GbGS1a* transcripts was higher in the leaves than in the other organs, it was four times  
199 lower than that of *GbGS2*. The three genes encoding *GbGS1b* were expressed at a higher level in  
200 the stems and roots than in the leaves. Two significant correlations were found: between the  
201 expression levels of *GbGS1a* and *GbGS2* (0.9) and those of *GbGS1b.1* and *GbGS1b.2* (0.89).

202 When fully expanded leaves were used, *GbGS1a* exhibited the highest level of expression compared  
203 to all the other GS genes during the L/D cycle. The pattern of *GbGS2* gene expression was similar

204 to that of *GbGS1a*, although the transcript accumulation was three times lower. Transcripts for  
205 *GbGS1b.3* were not detected irrespective of the light/dark regime (Figure 4B).  
206 *M. grandiflora* seedlings were also exposed to different light treatments to study the GS gene  
207 expression pattern in this species (Figure 5). The transcripts of *MgGS1a* and *MgGS2* were more  
208 abundant in leaves than in stems and roots, and their amounts were similar for *MgGS1a* in the L/D  
209 cycle and light-dark treatments. A very low level of expression was obtained for *MgGS1a* when  
210 seedlings were placed under continuous darkness. Its level of expression was approximately 4-fold  
211 lower than that of the L/D and light/dark treatments following a dark-light transition. *MgGS2* and  
212 *MgGS1a* exhibited a similar pattern of transcript accumulation, except that for the former, there was  
213 a significant decrease in the light-dark treatment and an increase during the transfer from dark to  
214 light. *MgGS1b.1* was the gene exhibiting the highest level of expression compared to all the other  
215 genes encoding GS. Its pattern of expression in the different organs was similar to that of *MgGS2*.  
216 However, the amounts of *MgGS1b.1* transcripts were much higher in the stems, notably in the L/D  
217 conditions, and in the roots. *MgGS1b.2* expression levels were similar in the three organs. No  
218 marked differences between the light and dark treatments were observed for this gene. *MgGS1b.3*  
219 transcript accumulation was similar irrespective of the organ and light/dark regimes, except in the  
220 stem, in which it was much higher during the L/D cycle. As shown in Figure 5, only four significant  
221 correlations were found between the expression level of the gene encoding GS in magnolia, where  
222 the highest correlation was between *MgGS1a* and *MgGS2* (0.92).

223

## 224 **DISCUSSION**

225 In all plant species, each GS isoenzyme plays a key role either in primary N assimilation or N  
226 recycling, as most of the N-containing molecules required for growth and development are derived  
227 from glutamine, the product of the reaction catalyzed by this enzyme. Throughout evolution, such  
228 important metabolic functions are subjected to a high selective pressure, which made GS  
229 particularly suitable for plant phylogenetic analyses. However, our knowledge of the phylogeny of a  
230 number of GS isoenzymes gathered in the evolutionary group called GSII remains limited. The aim  
231 of the present study was thus to improve our knowledge on the classification and phylogeny of the  
232 Viridiplantae GSII. This study was performed using the corresponding gene sequences belonging to  
233 the main clades that are representative of plant evolution and covering a large portfolio of species,  
234 not limited to the model and crop angiosperms.

235 In the present investigation, the resulting phylogenetic analysis agreed with previous studies in  
236 which two main groups of plant GSII encoded by nuclear genes were identified, namely, GSIIb  
237 (GLN2) and GSIIe (GLN1/GS) (Figures 1 and 2). An HGT event from eubacteria was previously



238 proposed as the more parsimonious process for the emergence of the GLN2 group (Tateno et al.  
239 1994; Ghoshroy et al. 2010). This hypothesis is further supported by the fact that we identified a  
240 signal peptide in all the GLN2 that allows the targeting of the proteins to organelles such as plastids  
241 and mitochondria (Table S1). Interestingly, genes encoding GLN2 were not identified in vascular  
242 plant (tracheophyte) species. Therefore, GLN2 seemed to be lost, coinciding with the final  
243 adaptation of plants to land habitats. Such an adaptive mechanism notably included the  
244 development of vascular structures for assimilate transport and the presence of lignin involved in  
245 plant stature (Raven 2018; Renault et al. 2019). In fact, the massive production of lignin, a  
246 metabolic feature of vascular plants, was enabled by a deregulation of phenylalanine biosynthesis  
247 that occurred at some point during the evolution of nonvascular plants and tracheophytes (El-Azaz  
248 et al. 2021). These developmental and regulatory processes could also be related to the selection of  
249 the GLN1/GS genes in the most ancient vascular plants. Thus, it was hypothesized that GLN1/GS  
250 isoenzymes are involved 1) in the synthesis of the transport of glutamine and derived amino acids  
251 (Bernard and Habash 2009), and 2) in the production of monolignols used as precursors for lignin  
252 biosynthesis. As lignin represents one of the main sinks for the photosynthetic carbon assimilated  
253 by the plant, high levels of GS activity are thus required to assimilate the large amounts of  
254 ammonium released during the reaction catalyzed by the enzyme phenylalanine ammonia-lyase  
255 (Pascual et al. 2016). The phylogenetic analyses performed in the present study suggested that the  
256 group represented by GLN1 isoenzymes can be considered the starting point for the evolution of the  
257 most recent genes encoding GS in plants.

258 The phylogeny of the ancient Embryophyta clades (Anthocerotophyta, Marchantiophyta and  
259 Bryophyta) suggested that the current GS subgroups in Spermatophyta clades were not established  
260 in nonvascular land plants (Figures 1 and 2). Curiously, GLN2 was also found in these three clades,  
261 which could be the result of a stable situation related to the interaction of genotypic and  
262 environmental conditions during the expansion of this group of plants. However, different  
263 clustering of GS in Lycopodiopsida and Polypodiopsida was observed between gene and protein  
264 phylogenetic trees, resulting in an unclear phylogenetic relationship (Figures 1 and 2). This finding  
265 suggests that during plant evolution, there was an active adaptation process as the result of changes  
266 in environmental conditions such as the increase in the  $O_2/CO_2$  ratio (Renault et al. 2019) and the  
267 loss of the *GLN2* gene. According to this hypothesis, several Lycopodiopsida and Polypodiopsida  
268 GS protein sequences contain a predicted transit peptide allowing its import into plastids (Table  
269 S1). Therefore, under an oxygen-enriched atmosphere, the occurrence of plastidic GS seems to be  
270 beneficial for the plant, in turn leading to positive selection.

271 We also refined the classification of GS in seed plants (Spermatophyta), leading to the identification  
272 of three distinct clusters. One was the well-known group of genes from angiosperms encoding  
273 plastidic GS (GS2) (see Hirel and Krapp 2021, for a review). The two other clusters contained the  
274 genes encoding cytosolic GS (GS1). In one of them, there were all the GS1 isoenzymes classically  
275 found in angiosperms and the GS1b from gymnosperms (Cánovas et al. 2007; Bernard and Habash  
276 2009). The third group included the GS1a from gymnosperms, including ginkgo, (Cantón et al.  
277 1993, Ávila-Sáez et al. 2000) and different GS1 from basal angiosperms and some Magnoliidae  
278 species. We thus propose to modify the nomenclature of GS from spermatophyte species into three  
279 types of genes, namely, GS1a, GS1b and GS2. Consequently, GSIIe can be used as a good  
280 phylogenetic marker in seed plants, since the presence or absence of the different GS gene groups is  
281 characteristic of the main taxa.

282 Surprisingly, searches for GS sequences in the NGS data from public databases allowed to identify  
283 genes encoding GS2 in Cycadopsida species, contrary to previous findings (Miyazawa et al. 2018).  
284 Such a finding was experimentally confirmed by cloning a cDNA encoding GS2 from *Cycas*  
285 *revoluta* (MZ073670). The obtained sequence of the cloned GS2 cDNA from *C. revoluta* validated  
286 the assembly of the *Cycas hainanensis* sequence using public NGS data (Figures S3 and S4).  
287 Consequently, this result demonstrated that there are more plant clades that possess GS2, which  
288 forms a new perspective on the evolution of GS2. In line with such a finding, recent phylogenomic  
289 studies showed that Cycadopsida and Ginkgoopsida formed a monophyletic group (Wu et al. 2013;  
290 Li et al. 2017; One Thousand Plant Transcriptomes Initiative 2019). The presence of the genes  
291 encoding GS2 in both clades and its absence in the other gymnosperm clades (Coniferopsida and  
292 Gnetopsida) supports this taxonomic classification.

293 Based on our phylogenetic analysis, two hypotheses can be proposed concerning GS2 emergence  
294 and evolution: 1) A two-event evolutionary process in which the gene encoding GS2 arose from a  
295 common ancestor of gymnosperms and angiosperms (Figure 6A). GS1 from Polypodiopsida, which  
296 is more closely related to GS2, could have been the origin of the plastid isoform following a  
297 specialization process that included the addition of a sequence that allowed the protein to be  
298 addressed into the plastids. This hypothesis implies that there was a second genetic event consisting  
299 of the loss of GS2 in the common ancestor of Coniferopsida and Gnetopsida plants. 2) A single  
300 event during which GS2 sequences emerged from a common ancestor of  
301 Cycadopsida/Ginkgoopsida and angiosperm clades, leaving Coniferopsida and Gnetopsida without  
302 this gene (Figure 6B). Although gymnosperms are considered a monophyletic clade that is sister to  
303 angiosperms (One Thousand Plant Transcriptomes Initiative 2019), the single-event hypothesis

304 about GS2 evolution is more parsimonious and suggests a revision of the phylogenetic relationships  
305 of the Cycadopsida/Ginkgoopsida clade with angiosperms.

306 The occurrence of a gene encoding GS1a has never been previously described in ginkgo, basal  
307 angiosperms, and a number of Magnoliidae species. The physiological function of GS1a was  
308 extensively studied in conifers because it compensates for the lack of GS2. Although GS1a is a  
309 cytosolic form of the enzyme, its light-dependent expression level is also associated with  
310 chloroplast development, photorespiration and N assimilation and recycling in photosynthetic  
311 tissues (Cánovas et al. 2007). One can hypothesize that, even though they are located in different  
312 cellular compartments, GS1a and GS2 play redundant roles in photosynthetic cells, which could  
313 explain the disappearance of GS1a in the most recent angiosperm species. The light dependence and  
314 organ gene expression of GS1a and GS2 in *P. pinaster* (Figure 3), *G. biloba* (Figure 4) and *M.*  
315 *grandiflora* (Figure 5) strengthened the previous hypothesis that GS1a fulfills the function of GS2  
316 (Cantón et al. 1999; Ávila et al. 2001; Gómez-Maldonado et al. 2004). Interestingly, one of the two  
317 Cys residues involved in the redox modulation of GS2 activity (e.g., C306 in *Arabidopsis*) was  
318 conserved in all the GS1a proteins (Cantón et al., 1993; Choi et al. 1999; Miyazawa et al. 2018).  
319 We also observed that this residue was conserved in all the GS1a and GS2 protein sequences  
320 analyzed in this study and in those from Polypodiopsida (ancient Embryophyta clades), a number of  
321 Lycopodiopsida species and in GLN1 sequences (Figure S5). Remarkably, this Cys is absent in all  
322 GS1b, suggesting a specific role of this residue in the function of GS2 and GS1a. In angiosperms, a  
323 second Cys residue is present in GS2 (e.g., C371 in *Arabidopsis*) and in a number of GLN1  
324 proteins. Moreover, this second Cys residue is not present in ginkgo or Cycadopsida GS2, which  
325 suggests that it was acquired by angiosperms during plant evolution (Figure S5).

326 When the single-event hypothesis is considered, the emergence of GS2 following the loss of GS1a  
327 in recent angiosperms indicates that they probably have redundant physiological functions. The  
328 Cycadopsida/Ginkgoopsida group emerged at least 270 mya ago (Wu et al. 2013; Li et al. 2017;  
329 One Thousand Plant Transcriptomes Initiative 2019) during the Permo-Carboniferous period, when  
330 the atmospheric oxygen level rose from 21 to 35%. Such an elevation in oxygen level led to a  
331 drastic increase in the oxygenase activity of the photosynthetic enzyme Rubisco, leading to  
332 increased photorespiration (Berling and Berner, 2000). The series of events that occurred during the  
333 Permo-Carboniferous period could result in the appearance of a plastidic GS isoenzyme (GS2) *via* a  
334 positive selection process, allowing for a more efficient reassimilation of ammonium that is released  
335 during photorespiration. Mutation of GS2 in a number of species induced lethality under  
336 photorespiratory conditions (Wallsgrave et al. 1987; Blackwell et al. 1987; Pérez-Delgado et al.  
337 2015), which is not the case in *Arabidopsis*, as it that can cope with the toxicity of ammonium

338 released from the photorespiratory pathway (Ferreira et al. 2019; Hachiya et al. 2021). Conifers,  
339 which are C3 species possessing only cytosolic GS isoenzymes (Figure 6C), are also able to  
340 reassimilate the ammonium released during photorespiration. However, the increase in the amount  
341 of atmospheric oxygen during the Permo-Carboniferous would imply an increase in nitrification  
342 rates, since oxygen is a substrate for nitrification (Ward, 2008), thus leading to an increase in nitrate  
343 availability in the rhizosphere. One can therefore hypothesize that such an increase in nitrate  
344 availability induced additional evolutionary pressure toward the selection of plastidic GS (GS2),  
345 which, in addition to photorespiratory ammonium reassimilation, is also responsible for the  
346 assimilation of ammonium in plastids derived from nitrate reduction (Figure 6D) (Hirel and Krapp  
347 2021). Consistent with this hypothesis, it is known that most conifers prefer or tolerate ammonium  
348 as an inorganic N source, which can be readily assimilated by cytosolic GS in the absence of GS2.  
349 Concerning the process of GS2 selection, the most likely hypothesis is the duplication of genes  
350 encoding cytosolic GS leading to functional specialization due to changes such as those in the gene  
351 promoter and the addition of a sequence encoding a signal peptide used to import the protein into  
352 the chloroplasts (Biesiadka and Legocki 1997, Ávila-Sáez et al. 2000). Gene expression patterns,  
353 specific Cys residue conservation and nucleotide sequence-based GS phylogeny suggest that GS1a  
354 could be at the origin of GS2 (Figures 1, 3-5).

355 Finally, we were able to conclude that the group represented by GS1b evolved in a different way  
356 than that grouping GS1a and GS2. In ginkgo and angiosperms, GS1b is generally represented by a  
357 small multigene family, with each member playing distinct roles either in N assimilation or N  
358 recycling, depending on the organ examined (Thomsen et al. 2014). In contrast, there is usually  
359 only one gene of GS1a or GS2, strongly suggesting that GS1b genes play nonredundant roles  
360 compared to GS1a and GS2 (Ghoshroy et al., 2010; Hirel and Krapp 2021). Related to their  
361 different roles, the comparison between the GS1a and GS1b proteins in pine showed distinctive  
362 characteristics, such as a higher thermal stability of GS1b (de la Torre et al. 2002).

363

## 364 **Conclusions**

365 The combined phylogenetic analysis and gene expression study presented in this work allowed us to  
366 improve our understanding of GS evolution in plants, notably in the Spermatophyta clade. In  
367 agreement with previous studies, two distinct groups of GS, GSIIb (GLN2) and GSIIe (GLN1 and  
368 GS), were clearly identified (Tateno et al. 1994; Ghoshroy et al. 2010).

369 An original finding of our study was that in seed plants, GS is represented by three types of genes  
370 (GS1a, GS1b and GS2), which allowed us to redefine the nomenclature of GS1 isoenzymes. In  
371 particular, the taxa possessing a gene encoding GS1a that was originally represented by conifers

372 (Cantón et al. 1993, 1999), are now expanded to ginkgo, basal angiosperms, and some Magnoliidae  
373 species. In contrast, GS1a is not present in the most recent angiosperm species such as monocots  
374 and eudicots. Therefore, GS1a represents a new functional group as this cytosolic GS isoenzyme is  
375 able to compensate for the lack of GS2 (Ávila et al. 2001).

376 Unexpectedly, a gene encoding GS2 was identified in Cycadopsida species. This new finding  
377 supports that this clade, together with Ginkgoopsida species, represents a monophyletic group (Wu  
378 et al. 2013). Concerning the emergence and evolution of GS2, we provide strong lines of evidence  
379 that this gene arose in the most recent common ancestor of Cycadopsida, Ginkgoopsida and  
380 angiosperms. However, additional analyses including GS gene sequences from ferns will be  
381 required to confirm this hypothesis.

382 Beyond the numerous studies already performed on crops, the present investigation proposes new  
383 possibilities toward a better understanding of the evolution of GS genes and their functions in  
384 terrestrial plants. Additional studies of GS evolution could help further deciphering the impact of  
385 the different GS isoenzymes on N use efficiency to improve plant growth and productivity under a  
386 wide range of environmental conditions.

387

## 388 **MATERIALS AND METHODS**

### 389 **Glutamine synthetase gene sequences and phylogenetic analyses**

390 Nucleotide sequences of the genes encoding plant glutamine synthetase type II (GSII) were  
391 obtained from different public databases or assembled from transcriptomic NGS data from SRA  
392 database at the National Center for Biotechnology Information (NCBI) and at the European  
393 Nucleotide Archive (EBI) (Table S1). The tool employed for sequence search was BLAST  
394 (Altschul et al. 1990) using mainly the *tblastn* mode with the sequence of GS1b.1 from *Pinus taeda*  
395 as the query. For the assembly of sequences from NGS data, the raw files were uploaded to the web  
396 platform Galaxy (<https://usegalaxy.org/>), which was used to make the transcriptome assemblies  
397 (Afgan et al. 2016). The raw reads were quality trimmed with the Trimmomatic software (Bolger et  
398 al. 2014). The transcriptome assemblies were conducted with the Trinity assembler (Grabherr et al.  
399 2011) and the GS sequences were identified using BLAST as described above. Database identifiers,  
400 names and species for the different GS sequences are presented in Table S1. All nucleotide  
401 sequences used in the present work are shown in Dataset S1. The subcellular localization prediction  
402 was determined with TargetP (Almagro Armenteros et al. 2019) and LOCALIZER software  
403 (Sperschneider et al. 2017).

404 For Bayesian phylogenetic analysis a dataset of 169 nucleotide sequences encoding GSII from 45  
405 different Viridiplantae species and *glnA* from *Escherichia coli* were aligned with the Muscle

406 software (Edgar, 2004). Position with gaps were deleted, and MRMODELTEST v2.4 was used to  
407 find the best fit model among 24 models used to study molecular evolution (Nylander, 2004). The  
408 Akaike Information Criterion suggested to use model GTR+I+G. The Bayesian phylogenetic  
409 analysis was performed using MRBAYES v3.2.7 (Huelsenbeck and Ronquist, 2001) with two  
410 simultaneous runs of 77 million generations for each run, with one cold and three heated chains for  
411 each run in which the temperature parameter was set to 0.1. Trees were sampled once every 10,000  
412 generations. The average standard deviation of split frequencies at the end of each run was < 0.01,  
413 and the first 25 % of the trees were discarded as burn-in samples. The consensus tree was visualized  
414 with the interactive Tree Of Life (iTOL) web tool (Letunic and Bork 2019).  
415 For maximum likelihood analysis the dataset composed of 169 GS protein sequences obtained from  
416 the corresponding nucleotide sequences that were used for the Bayesian analyses. The alignment  
417 and phylogenetic analysis were conducted using MEGA7 (Kumar et al. 2016). The sequences were  
418 aligned with Muscle (Edgar, 2004). Maximum likelihood analyses were carried out using the  
419 complete deletion of gaps, the missing data, and the amino acid substitution model Jones-Taylor-  
420 Thornton (JTT) (Jones et al. 1992). The Nearest-Neighbor-Interchange (NNI) was used for tree  
421 inference. The initial tree was constructed using the NJ/BioNJ method. The phylogeny test was  
422 performed using the Bootstrap method with 1,000 replications.

423

#### 424 **Plant material**

425 *G. biloba* seeds were obtained from different botanic gardens: Botanische Gärten der Universität  
426 Bonn (Bonn, Germany), Botanischer Garten der Universität Bern (Bern, Switzerland), Plantentuin  
427 Universteit Gent (Ghent, Belgium) and Arboretum Wespelaar (Wespelaar, Belgium). Ginkgo seeds  
428 were stratified for 3 months in vermiculite at 4°C. *P. pinaster* seeds from Sierra Bermeja (Estepona,  
429 Spain) (ES20, Ident. 11/12) were obtained from the *Red de Centros Nacionales de Recursos*  
430 *Genéticos Forestales* of the Spanish *Ministerio para la Transición Ecológica y el Reto*  
431 *Demográfico* with the authorization number ESNC87. Pine seeds were imbibed for 72 hours under  
432 continuous aeration with an air pump. *M. grandiflora* seeds were obtained from the Parque de la  
433 Alameda garden in Málaga (Spain) and from private suppliers. Magnolia seeds were stratified in  
434 vermiculite at 4°C for 4 months. All seeds were growth on vermiculite in order to prevent any  
435 nutritional effect of the substrate.

436 Ginkgo, pine, and magnolia seedlings were germinated and grown at 23°C either with a 16h light/8h  
437 dark photoperiod and watered once every 3 days with distilled water or under continuous darkness  
438 and watered once a week. For light/dark transition experiments, seedlings grown in complete  
439 darkness were transferred to a 16h light/8h night photoperiod for 24 hours and seedlings grown with

440 16h light/8h night were transferred to complete darkness for 24 hours. Leaves, stems, and roots of  
441 seedlings were harvested separately. For ginkgo seedlings grown in complete darkness, primary and  
442 secondary leaves were not developed, thus only stems and roots were harvested. To study the  
443 impact of a light-dark transition on the expression of the different genes encoding GS in ginkgo  
444 leaves, one-year old plants with fully developed leaves were used. These plants were first exposed  
445 to a 16h light /8h night photoperiod, then to complete darkness for 24 hours and then back to a 16h  
446 light /8h night cycle. The different plant samples were immediately frozen in liquid N and stored at  
447 -80°C.

448 For the cloning of *Cycas revoluta* GS2, leaves from a one-year-old plants grown under 16h light/8h  
449 night photoperiod were harvested. Leaf tissues were frozen immediately in liquid N and stored at -  
450 80°C until further use for RNA extraction.

451

#### 452 **RNA extraction and RT-qPCR**

453 Ginkgo and magnolia RNAs were extracted using the Plant/Fungi Total RNA Purification Kit  
454 (Norgen Biotek Corp., Thorold, ON, Canada) according to the manufacturer's instruction manual.  
455 Pine and *Cycas* RNAs were extracted as described by Canales et al. (2012). For the cDNA  
456 synthesis, 500 ng of total RNA were used and retrotranscribed using the iScript<sup>TM</sup> Reverse  
457 Transcription Supermix (Bio-Rad, Hercules, CA, USA). qPCR was carried out using 10 ng of  
458 cDNA and the SsoFast<sup>TM</sup> EvaGreen® Supermix (Bio-Rad, Hercules, CA, USA). The reaction was  
459 carried out in a thermal cycler CFX384<sup>TM</sup> Touch Real-Time PCR (Bio-Rad, Hercules, CA, USA).  
460 The results for maritime pine were normalized using a *saposin-like aspartyl protease* (unigene1135)  
461 as a reference gene (Granados et al. 2016). A number of references genes used to study gene  
462 expression in maritime pine (Granados et al. 2016) were tested in ginkgo and magnolia. In this  
463 species, the orthologs of maritime pine *saposin-like aspartyl protease* (unigene1135), *myosin heavy*  
464 *chain-related* (unigene13291) and of an RNA binding protein (unigene27526) were selected and  
465 used to normalize the expression of the genes encoding GS. In magnolia, the ortholog of an *RNA*  
466 *binding protein* (unigene27526) from maritime pine and *Actin-7* from magnolia (Lovisetto et al.  
467 2015) were selected and used as reference genes. The different primers used for the RT-qPCR  
468 experiments are presented in Table S2. Magnolia and ginkgo sequences used to design the primers  
469 are listed in Table S3.

470 A GS2 cDNA from *C. revoluta* was cloned using a PCR product. An iProof<sup>TM</sup> HF Master Mix (Bio-  
471 Rad, Hercules, CA, USA) was used to perform the PCR reaction. Primer sequences were obtained  
472 from *C. hainanensis* and presented in Table S2. After the initial denaturation step at 98°C during 1  
473 min, the PCR was conducted during 35 cycles with the following conditions: 10 s at 98°C; 20 s at

474 60°C and 1 min at 72°C, with a final extension step at 72°C for 5 min. The resulting PCR product  
475 was cloned into the pJET1.2 cloning vector (Thermo, Waltham, MA, USA). The sequence of GS2  
476 from *C. revoluta* was submitted to Genbank (MZ073670).

477

#### 478 **Statistics**

479 Statistical analyses were performed using Prism 8 (Graphpad, CA, USA). Data obtained from gene  
480 expression quantification were analyzed using a multiple comparison Two-Way Anova test.  
481 Differences between organs were not analyzed statistically. The Tukey's test was used as a post hoc  
482 test for statistical analysis of the gene expression data. For *G. biloba* and *M. grandiflora* seedlings a  
483 Pearson correlation test was also used to evaluate the relationship existing between the expressions  
484 of the different *GS* genes. Differences and correlations were considered to be significant when the  
485 *p*-value was < 0.05.

486

#### 487 **ACKNOWLEDGEMENTS**

488 The authors are very grateful to Dr. Juan Antonio Pérez Claros for his helpful comments on the  
489 manuscript and Anett Krämer (Botanische Gärten der Universität Bonn, Germany), Katja Rembold  
490 (Botanischer Garten der Universität Bern, Switzerland), Chantal Dugardin (Plantentuin Universteit  
491 Gent, Belgium) and Joke Ossaer (Arboretum Wespelaar, Belgium) for the kind supply of ginkgo  
492 seeds. We are also very grateful to José Manuel Sánchez Calle and María Dolores Trujillo Gutiérrez  
493 for the kind supply of magnolia seeds. This work was supported by Spanish *Ministerio de Ciencia e*  
494 *Innovación*, grant numbers BIO2015-73512-JIN MINECO/AEI/FEDER, UE; RTI2018-094041-B-  
495 I00 and EQC2018-004346-P. This work was also supported by *Junta de Andalucía*, grant number  
496 P20\_00036 PAIDI 2020/FEDER, UE. JMVM was supported by a grant from the Spanish *Ministerio*  
497 *de Educación y Formación Profesional* (FPU17/03517). FO was supported by grants from the  
498 *Universidad de Málaga (Programa Operativo de Empleo Juvenil vía SNJG, UMAJ111, FEDER,*  
499 *FSE, Junta de Andalucía)* and BIO-114, *Junta de Andalucía*.

500

#### 501 **AUTHORS CONTRIBUTION**

502 JMVM and FO have performed the experiments; FRC and RAC have performed the phylogenetic  
503 analysis; JMVM, BH, FRC and RAC have wrote the manuscript; JMVM, FO and RAC have design  
504 the figures; FMC and CA have made additional contributions and edited the manuscript. RAC, CA,  
505 and FMC were responsible of the funding acquisition; FRC and RAC have planned and designed  
506 the research.



507 **DATA AVAILABILITY**

508 The data that support the findings of this study are available from different databases, supporting  
509 information and from the corresponding author upon reasonable request.

510

511 **CONFLICTS OF INTEREST**

512 The authors declare no conflict of interest.

513

514 **REFERENCES**

515 Afgan E, Baker D, Batut B, van den Beek M, Bouvier D, Čech M, Chilton J, Clements D, Coraor N,  
516 Grüning B, et al. 2018. The Galaxy platform for accessible, reproducible and collaborative  
517 biomedical analyses: 2018 update. *Nucleic Acids. Res.* 46:W537-W544.

518 Almagro Armenteros JJ, Salvatore M, Emanuelsson O, Winther O, von Heijne G, Elofsson A,  
519 Nielsen H. 2019. Detecting sequence signals in targeting peptides using deep learning. *Life Sci.*  
520 *Alliance* 2:e201900429.

521 Amiour N, Décousset L, Rouster J, Quenard N, Buet C, Dubreuil P, Quilleré I, Brulé L, Cukier C,  
522 Dinant S, et al. 2021. Impacts of environmental conditions, and allelic variation of cytosolic  
523 glutamine synthetase on maize hybrid kernel production. *Commun Biol.*4:1095.

524 Altschul SF, Gish W, Miller W, Myers EW, Lipman DJ. 1990. Basic local alignment search tool. *J.*  
525 *Mol. Biol.* 215:403-410.

526 Ávila-Sáez C, Muñoz-Chapuli R, Plomion C, Frigerio J, and Cánovas FM. 2000. Two genes  
527 encoding distinct cytosolic glutamine synthetases are closely linked in the pine genome. *FEBS Lett.*  
528 477:237-43.

529 Ávila C, Suárez MF, Gómez-Maldonado J, and Cánovas FM. 2001. Spatial and temporal expression  
530 of two cytosolic glutamine synthetase genes in Scots pine: functional implications on nitrogen  
531 metabolism during early stages of conifer development. *Plant J.* 25:93-102.

532 Berling DJ, Berner RA. 2000. Impact of a Permo-Carboniferous high O<sub>2</sub> event on  
533 the terrestrial carbon cycle. *Proc. Nat. Acad. Sci. U.S.A.* 97:12428-12432.

534 Bernard SM, Habash DZ. 2009. The importance of cytosolic glutamine synthetase in nitrogen  
535 assimilation and recycling. *New Phytol.*182:608-620.

536 Biesiadka J, Legocki AB. 1997. Evolution of the glutamine synthetase gene in plants. *Plant Sci.*  
537 128: 51-58.

538 Birol I, Raymond A, Jackman S.D, Pleasance S, Coope R, Taylor G.A, Yuen MMS, Keeling CI,  
539 Brand D, Vandervalk BP, et al. 2013. Assembling the 20 Gb white spruce (*Picea glauca*) genome  
540 from whole-genome shotgun sequencing data. *Bioinformatics* 29 12:1492-1497.

- 541 Bolger AM, Lohse M, Usadel B. 2014. Trimmomatic: A flexible trimmer for Illumina Sequence  
542 Data. *Bioinformatics* 30: 2114-2120.
- 543 Blackwell RD, Murray AJS, Lea PJ. 1987. Inhibition of photosynthesis in barley with decreased  
544 levels of chloroplastic glutamine synthetase activity. *J. Exp. Bot.* 196:1799-1809.
- 545 Canales J, Rueda-López M, Craven-Bartle B, Avila C, Cánovas FM. 2012. Novel insights into  
546 regulation of asparagine synthetase in conifers. *Front. Plant Sci.* 24:3-100.
- 547 Cánovas FM, Avila C, Cantón FR, Cañas RA, de la Torre F. 2007. Ammonium assimilation and  
548 amino acid metabolism in conifers. *J. Exp. Bot.* 58:2307-2318.
- 549 Cantón FR, García-Gutiérrez A, Gallardo F, de Vicente A, Cánovas FM. 1993. Molecular  
550 characterization of a cDNA clone encoding glutamine synthetase from a gymnosperm, *Pinus*  
551 *sylvestris*. *Plant Mol. Biol.* 22:819-828.
- 552 Cantón FR, Suárez MF, Josè-Estanyol M, Cánovas FM. 1999. Expression analysis of a cytosolic  
553 glutamine synthetase gene in cotyledons of Scots pine seedlings: developmental, light regulation  
554 and spatial distribution of specific transcripts. *Plant. Mol. Bio.* 404:623-34.
- 555 Choi YA, Kim SG, Kwon YM. 1999. The plastidic glutamine synthetase activity is directly  
556 modulated by means of redox change at two unique cysteine residues. *Plant Sci.* 149:175-182.
- 557 de la Torre F, García-Gutiérrez A, Crespillo R, Cantón FR, Avila C, Cánovas FM. 2002. Functional  
558 expression of two pine glutamine synthetase genes in bacteria reveals that they encode cytosolic  
559 holoenzymes with different molecular and catalytic properties. *Plant Cell Physiol.* 437:802-809.
- 560 Edgar R. C. 2004. MUSCLE: multiple sequence alignment with high accuracy and high throughput.  
561 *Nucleic Acids Res.* 32:1792-1797.
- 562 El-Azaz J, Cánovas FM, Barcelona B, Avila C, de la Torre F. 2021. Deregulation of phenylalanine  
563 biosynthesis evolved with the emergence of vascular plants. *Plant Physiol.* (forthcoming)  
564 doi:10.1093/plphys/kiab454.
- 565 Ferreira S, Moreira E, Amorim I, Santos C, Melo P. 2019. *Arabidopsis thaliana* mutants devoid of  
566 chloroplast glutamine synthetase (GS2) have non-lethal phenotype under photorespiratory  
567 conditions. *Plant Physiol. Biochem.* 144:365-374.
- 568 García-Gutiérrez A, Dubois F, Cantón FR, Gallardo F, Sangwan RS, and Cánovas F. 1998. Two  
569 different models of early development and nitrogen assimilation in gymnosperm seedlings. *Plant J.*  
570 132:187-199.
- 571 Granados JM, Ávila C, Cánovas FM, Cañas RA. 2016. Selection and testing of reference genes for  
572 accurate RT-qPCR in adult needles and seedlings of maritime pine. *Tree Genet. Genomes*12:60-75.

- 573 Ghoshroy S, Binder M, Tartar A, Robertson DL. 2010. Molecular evolution of glutamine synthetase  
574 II: phylogenetic evidence of a non-endosymbiotic gene transfer event early in plant evolution. *BMC*  
575 *Evol. Biol.*10:198.
- 576 Gómez-Maldonado J, Avila C, de la Torre F, Cañas R, Cánovas FM, Campbell MM. 2004.  
577 Functional interactions between a glutamine synthetase promoter and MYB proteins. *Plant J.*  
578 39:513-26.
- 579 Grabherr MG, Haas BJ, Yassour M, Levin JZ, Thompson DA, Amit I, Adiconis X, Fan L,  
580 Raychowdhury R, Zeng Q, et al. 2011. Full-length transcriptome assembly from RNA-seq data  
581 without a reference genome. *Nat Biotechnol.* 29:644-652.
- 582 Guan R, Zhao Y, Zhang H, Fan G, Liu X, Zhou W, Shi C, Wang J, Liu W, Liang X, et al. 2016.  
583 Draft genome of the living fossil *Ginkgo biloba*. *Gigascience* 5:49.
- 584 Hachiya T, Inaba J, Wakazaki M, Sato M, Toyooka K, Miyagi A, Kawai-Yamada M, Sugiura D,  
585 Nakagawa T, Kiba T, et al. 2021. Excessive ammonium assimilation by plastidic glutamine  
586 synthetase causes ammonium toxicity in *Arabidopsis thaliana*. *Nat. Commun.* 12:4944.
- 587 Heldt H, Piechulla B. 2011. Plant Biochemistry: fourth edition. San Diego: Academic Press,  
588 Elsevier.
- 589 Havé M, Marmagne A, Chardon F, Masclaux-Daubresse C. 2017. Nitrogen remobilization during  
590 leaf senescence: lessons from *Arabidopsis* to crops. *J. Exp. Bot.* 68:2513-2529.
- 591 Hirel B and Krapp A. 2021. Nitrogen Utilization in Plants I Biological and Agronomic Importance.  
592 *Encyclopedia of Biological Chemistry III (Third Edition)*. Editor: Joseph Jez, 1: 127–140. Elsevier.  
593 ISBN 9780128220405, doi:10.1016/b978-0-12-809633-8.21265-x.
- 594 Hu L, Xu Z, Wang M, Fan R, Yuan D, Wu B, Wu H, Qin X, Yan L, Tan L, et al. 2019. The  
595 chromosome-scale reference genome of black pepper provides insight into piperine biosynthesis.  
596 *Nat. Commun.* 10:4702.
- 597 Huelsenbeck JP, Ronquist F. 2001. MRBAYES: Bayesian inference of phylogeny. *Bioinformatics*  
598 17:754-755.
- 599 James D, Borphukan B, Fartyal D, Achary VMM, Reddy MK. 2018. Transgenic manipulation of  
600 glutamine synthetase: A target with untapped potential in various aspects of crop improvement. In:  
601 Gosal SS, Wani SH, editors. *Biotechnology of Crop Improvement*. Springer International  
602 Publishing AG. p. 367-416.
- 603 Jones DT, Taylor WR, Thornton JM. 1992. The rapid generation of mutation data matrices from  
604 protein sequences. *Comput. Appl. Biosci.* 8:275-282.
- 605 Krapp A. 2015. Plant nitrogen assimilation and its regulation: a complex puzzle with missing  
606 pieces. *Curr. Opin. Plant. Biol.* 25:115-122.

- 607 Kumada Y, Benson DR, Hillemann D, Hosted TJ, Rochefort DA,  
608 Thompson CJ, Wohlleben W, Tateno, Y. 1993. Evolution of the  
609 glutamine synthetase gene, one of the oldest existing and functioning genes.  
610 *Proc. Nat. Acad. Sci. U.S.A.* 90:3009-3013.
- 611 Kumar S, Stecher G, Tamura K. 2016. MEGA7: Molecular Evolutionary Genetics Analysis Version  
612 7.0 for Bigger Datasets. *Mol. Biol. Evol.* 33:1870-1874.
- 613 Kumar V, Yadav S, Soumya N, Kumar R, Babu NK, Singh S. 2017. Biochemical and inhibition  
614 studies of glutamine synthetase from *Leishmania donovani*. *Microb. Pathog.* 107:164-174.
- 615 Kuzmin DA, Ferachuk SI, Sharov VV, Cybin AN, Makolov SV, Putintseva A, Oreshkova NV,  
616 Krutovsky KV. 2019. Stepwise large genome assembly approach: a case of Siberian larch (*Larix*  
617 *sibirica* Ledeb). *BMC Bioinformatics* 20:37.
- 618 Lea PJ, Mifflin BJ. 2018. Nitrogen assimilation and its relevance to crop improvement. In: Foyer  
619 CH, Zhang H, editors. Annual Plant Reviews. Volume 42. Nitrogen Metabolism In Plants in the  
620 Post-Genomic Era. Chichester: Wiley-Blackwell, pp. 1-40.
- 621 Letunic I, and Bork P. 2019. Interactive Tree Of Life (iTOL) v4: recent updates and new  
622 developments. *Nucleic Acids Res.* 47: W256-W259.
- 623 Li Z, De La Torre AR, Sterck L, Cánovas FM, Avila C, Merino I, Cabezas JA, Cervera MT,  
624 Ingvarsson PK, Van de Peer Y. 2017. Single-Copy Genes as Molecular Markers for Phylogenomic  
625 Studies in Seed Plants. *Genome Biol. Evol.* 9:1130-1147.
- 626 Lovisetto A, Masiero S, Rahim MA, Mendes MA, Casadoro G. 2015. Fleshy seeds form in the  
627 basal Angiosperm *Magnolia grandiflora* and several MADS-box genes are expressed as fleshy seed  
628 tissues develop. *Evol Dev.* 1:82-91.
- 629 Mathis R, Gamas P, Meyer Y, Cullimore JV. 2000. The presence of  
630 GSI-like genes in higher plants: support for the paralogous evolution of GSI  
631 and GSII. *J. Mol. Evol.* 50:116-122.
- 632 Miyazawa SI, Nishiguchi M, Futamura N, Yukawa T, Miyao M, Maruyama TE, Kawahara T. 2018.  
633 Low assimilation efficiency of photorespiratory ammonia in conifer leaves. *J Plant Res.* 131:789-  
634 802.
- 635 Mondal R, Kumar A, Chattopadhyay SK. 2021. Structural property, molecular regulation and  
636 functional diversity of Glutamine Synthetase in higher plants: a data-mining bioinformatics  
637 approach. *Plant J.* (in press). doi: 10.1111/TPJ.15536
- 638 Mosca E, Cruz F, Gómez-Garrido J, Bianco L, Rellstab C, Brodbeck S, Csilléry K, Fady B, Flandug  
639 M, Fussi B, et al. 2019. A Reference Genome Sequence for the European Silver Fir (*Abies alba*  
640 mill.): A Community-Generated Genomic Resource. *G3 (Bethesda)* 9:2039-2049.

- 641 Neale DB, Wegrzyn JL, Stevens KA, Zimin AV, Puiu D, Crepeau MW, Cardeno C, Koriabine M,  
642 Holtz-Morris AE, Liechty JD, et al. 2014. Decoding the massive genome of loblolly pine using  
643 haploid DNA and novel assembly strategies. *Genome Biol.* 15:R59.
- 644 Neale DB, McGuire PE, Wheeler NC, Stevens KA, Crepeau MW, Careno C, Zimin AV, Puiu D,  
645 Perteau GM., Sezen UU, et al. 2017. The Douglas-Fir Genome Sequence Reveals Specialization of  
646 the Photosynthetic Apparatus in Pinaceae. *G3 (Bethesda)* 7:3157-3167.
- 647 Nogueira ED, Olivares FL, Japiassu JC, Vilar C, Vinagre F, Baldani JJ,  
648 Hemeryly AS. 2005. Characterization of glutamine synthetase genes in sugar cane genotypes with  
649 different rates of biological nitrogen fixation. *Plant. Sci.* 169:819-832.
- 650 Nylander JAA. 2004. MrModeltest v2. Program distributed by the author. Evolutionary Biology  
651 Centre, Uppsala University. <https://github.com/nylander/MrModeltest2>
- 652 Nystedt B, Street NR, Wetterbom A, Zuccolo A, Lin YC, Scofield DG, Vezzi F, Delhomme N,  
653 Giacomello S, Alexeyenko A, et al. 2013. The Norway spruce genome sequence and conifer  
654 genome evolution. *Nature.* 497:579-584.
- 655 One Thousand Plant Transcriptomes Initiative. 2019. One thousand plant transcriptomes and the  
656 phylogenomics of green plants. *Nature* 574:679-685.
- 657 Pascual MB, El-Azaz J, de la Torre FN, Cañas RA, Avila C, Cánovas FM. 2016. Biosynthesis and  
658 Metabolic Fate of Phenylalanine in Conifers. *Front. Plant Sci.* 7:1030.
- 659 Pérez-Delgado CM, García-Calderón M, Márquez AJ, Betti M. 2015. Reassimilation of  
660 Photorespiratory Ammonium in *Lotus japonicus* Plants Deficient in Plastidic Glutamine Synthetase.  
661 *PLoS One.* 10:e0130438.
- 662 Pesole G, Bozzetti MP, Lanave C, Preparata G, Saccone, C. 1991.  
663 Glutamine synthetase gene evolution: a good molecular clock. *Proc. Nat. Acad. Sci. U.S.A.* 88:522-  
664 526.
- 665 Plett D, Garnett T, Okamoto M. 2017. Molecular genetics to discover and improve nitrogen use  
666 efficiency in crop plants. In: Hossain MA, Kamiya T, Burritt DJ, Tran LSP, Fujiwara T, editors.  
667 Plant Macronutrient Use Efficiency. London: Academic Press, pp. 93-122.
- 668 Raven JA. 2018. Evolution and palaeophysiology of the vascular system and other means of long-  
669 distance transport. *Philos. Trans. R. Soc. Lond. B Biol. Sci.* 373:20160497
- 670 Renault H, Werck-Reichhart D, Weng JK. 2019. Harnessing lignin evolution for biotechnological  
671 applications. *Curr. Opin. Biotechnol.* 56:105-111.
- 672 Robertson DL, Tartar A. 2006. Evolution of glutamine synthetase in heterokonts: evidence for  
673 endosymbiotic gene transfer and the early evolution of photosynthesis. *Mol. Biol. Evol.* 23:1048-55.

- 674 Scott AD, Zimin AV, Puiu D, Workman R, Britton M, Zaman S, Caballero M, Read AC,  
675 Bogdanove AJ, Burns E, et al. 2020. A Reference Genome Sequence for Giant Sequoia. *G3*  
676 (*Bethesda*) 10:3907-3919.
- 677 Shatters RG, Kahn ML. 1989. Glutamine Synthetase II in *Rhizobium*: Reexamination of the  
678 Proposed Horizontal Transfer of DNA from Eukaryotes to Prokaryotes. *J. Mol. Evol.* 29: 422-428.
- 679 Sperschneider J, Catanzariti AM, DeBoer K, Petre B, Gardiner DM, Singh KB, Dodds PN, Taylor  
680 JM. 2017. LOCALIZER: subcellular localization prediction of both plant and effector proteins in  
681 the plant cell. *Sci. Rep.* 16:44598.
- 682 Stevens KA, Wegrzyn JL, Zimin A, Puiu D, Crepeau M, Cardeno C, Paul R, Gonzalez-Ibeas D,  
683 Koriabine M, Holtz-Morris AE, et al. 2016. Sequence of the Sugar Pine Megagenome. *Genetics*,  
684 204:1613-1626.
- 685 Tateno Y. 1994. Evolution of glutamine synthetase genes is in accordance with the neutral theory of  
686 molecular evolution. *Jpn J Genet* 69:489-502.
- 687 Tegeder M, Masclaux-Daubresse C. 2017. Source and sink mechanisms of nitrogen transport and  
688 use. *New Phytol.* 217:35-53.
- 689 Thomsen HC, Erikson D, MØller IS, Schjoerring, JK. 2014. Cytosolic glutamine synthetase: A  
690 target for improvement of crop nitrogen use efficiency? *Trends Plant Sci.* 19:656–663
- 691 Wallsgrove RM, Turner JC, Hall NP, Kendall AC, Bright SW. 1987. Barley mutants lacking  
692 chloroplast glutamine synthetase-biochemical and genetic analysis. *Plant Physiol* 83:155-158.
- 693 Wan T, Liu ZM, Li LF, Leitch AR, Leitch IL, Lohaus R, Liu ZJ, Xin HP, Huang JL, Li Z, et al.  
694 2018. A genome for gnetophytes and early evolution of seed plants. *Nat. Plants* 4:82-89.
- 695 Ward BB. 2008. Nitrification. In: Jørgensen SE, Fath BD, editors. *Encyclopedia of Ecology*.  
696 Amsterdam (The Netherlands): Elsevier Science. p. 2511-2518.
- 697 Wu CS, Chaw SW, Huang YY. 2013. Chloroplast Phylogenomics Indicates that *Ginkgo biloba* Is  
698 Sister to Cycads. *Genome Biol. Evol.* 5:243-254.
- 699 Xu G, Fan X, Miller AJ. 2012. Plant Nitrogen Assimilation and Use Efficiency. *Annu. Rev. Plant*  
700 *Biol.* 63:153-182.
- 701 Zimin A, Stevens KA, Crepeau MW, Holtz-Morris A, Koriabine M, Marçais G, Puiu D, Roberts M,  
702 Wegrzyn JL, de Jong PJ, et al. 2014. Sequencing and assembly of the 22-gb loblolly pine genome.  
703 *Genetics*, 196:875-90.

704

## 705 **FIGURE LEGENDS**

706 **Figure 1.** Phylogenetic tree of plant GS nucleotide sequences obtained following a Bayesian  
707 analysis. The first two letters of the sequence names correspond to genera and species listed in

708 Table S1. Green circles highlight the sequences exhibiting a predicted plastidic localization. Orange  
709 circles highlight the sequences exhibiting a predicted mitochondrial localization. Branch lengths are  
710 not presented.

711 **Figure 2.** Protein phylogenetic tree of plant GS protein sequences following a Maximum  
712 Likelihood analysis. The first two letters of the sequence names correspond to genera and species  
713 listed in Table S1. Green circles highlight the sequences with a predicted chloroplastic localization.  
714 Orange circles highlight the sequences with a predicted mitochondrial localization. Branch lengths  
715 are not presented.

716 **Figure 3.** *PpGS1a* and *PpGS1b* gene expression in *Pinus pinaster* seedlings grown under different  
717 light regimes. L/D cycle (16h light /8h dark photoperiod, red bars), light photoperiod to continuous  
718 darkness transition (orange bars), continuous darkness (yellow bars) and complete darkness to light  
719 photoperiod transition (blue bars). Significant differences were determined using Two-way  
720 ANOVA that compare the mean for each condition with the mean of the other condition in the same  
721 organ. Letters above the columns indicate significant differences when a Tukey's post-hoc test ( $p <$   
722 0.05) was applied.

723 **Figure 4.** GS gene expression in *Ginkgo biloba* seedlings grown under different light regimes.  
724 Panel **A.** One-month old seedlings under L/D cycle: 16h light /8h dark photoperiod (red bars) and  
725 continuous darkness (yellow bars). A Pearson correlation test was applied to the expression level of  
726 the different GS genes to quantify their relationship indicated in the red squares. The significant  $p$ -  
727 values ( $< 0.05$ ) for the Pearson coefficient are indicated in brackets. Panel **B.** One-year old  
728 seedlings under L/D cycle (16h light /8h dark photoperiod, red bars), light photoperiod to  
729 continuous darkness transition (orange bars) and complete darkness to light photoperiod transition  
730 (blue bars). Significant differences were determined using a two-way ANOVA to compare the mean  
731 for each growth condition with the mean of the other conditions in the same organ. Letters above  
732 the columns indicate significant differences based on a Tukey's post-hoc test ( $p < 0.05$ ). nd= non-  
733 detected; ms= missing sample.

734 **Figure 5.** GS gene expression in *Magnolia grandiflora* seedlings grown under different light  
735 regimes. L/D cycle (16h light /8h dark photoperiod, red bars), light photoperiod to continuous  
736 darkness transition (orange bars), continuous darkness (yellow bars) and complete darkness to light  
737 photoperiod transition (blue bars). Significant differences were determined using Two-way  
738 ANOVA that compare the mean for each condition with the mean of the other condition for the  
739 same organ. Letters above the columns indicate significant differences when a Tukey's post-hoc test  
740 ( $p < 0.05$ ) was applied. Correlations between the expression levels of the different genes expressed

741 in *M. grandiflora* using a Pearson Correlation test. The significant  $p$ -value ( $< 0.05$ ) are indicated in  
742 brackets.

743 **Figure 6.** Schematic representation of GS2 emergence hypotheses. **A.** Two-event hypothesis. **B.**  
744 Single-event hypothesis. **C.** Simplified metabolic pathways in a photosynthetic cell in which  
745 ammonium assimilation is catalyzed by GS1a. **D.** Metabolic pathway of a photosynthetic cell in  
746 which ammonium assimilation is catalyzed by GS2. GS, glutamine synthetase. Fd-GOGAT,  
747 ferredoxin dependent glutamate synthase. NR, nitrate reductase. NiR, nitrite reductase.

748

#### 749 **SUPPLEMENTAL DATA**

750 **Table S1.** Sequences names, accession numbers, species taxonomy data and putative subcellular  
751 localization of the different encoded GS.

752 **Table S2.** List of primers used for RT-qPCR experiments *CrGS2* cloning.

753 **Table S3.** Magnolia and ginkgo GS gene sequences used to design the primers used for RT-qPCR  
754 experiments.

755 **Dataset S1.** GS nucleotide sequences used to perform the phylogenetic analyses.

756 **Dataset S2.** GS protein sequences to perform the phylogenetic analyses.

757 **Dataset S3.** Detailed results of the Bayesian analysis using the GS gene nucleotide sequences.

758 **Dataset S4.** Detailed results of the maximum likelihood analysis using the GS protein sequences.

759 **Figure S1.** Phylogenetic tree obtained following a Bayesian analysis of the GS nucleotide  
760 sequences in which the branch lengths are maintained. Green circles correspond a predicted plastid  
761 localization of the corresponding protein. Orange circles correspond to a predicted mitochondrial  
762 localization.

763 **Figure S2.** Phylogenetic tree obtained following a Bayesian analysis of the GS protein sequences in  
764 which the branch lengths are maintained. Green circles correspond predicted plastid localization.  
765 Orange circles correspond to a predicted mitochondrial localization.

766 **Figure S3.** Multiple sequence alignment of the GS2 protein sequences from *Cycas revoluta*  
767 (*CrGS2*) and *Cycas hainanensis* (*ChaGS2*).

768 **Figure S4.** Multiple sequence alignment of the complete coding sequences (CDS) of the genes  
769 encoding GS2 from *Cycas revoluta* (*CrGS2*) and *Cycas hainanensis* (*ChaGS2*).

770 **Figure S5.** Multiple sequence alignment of the protein regions around the Cys residues involved in  
771 the redox modulation of GS2 activity, C306 and C371 positions in *Arabidopsis* GS2.



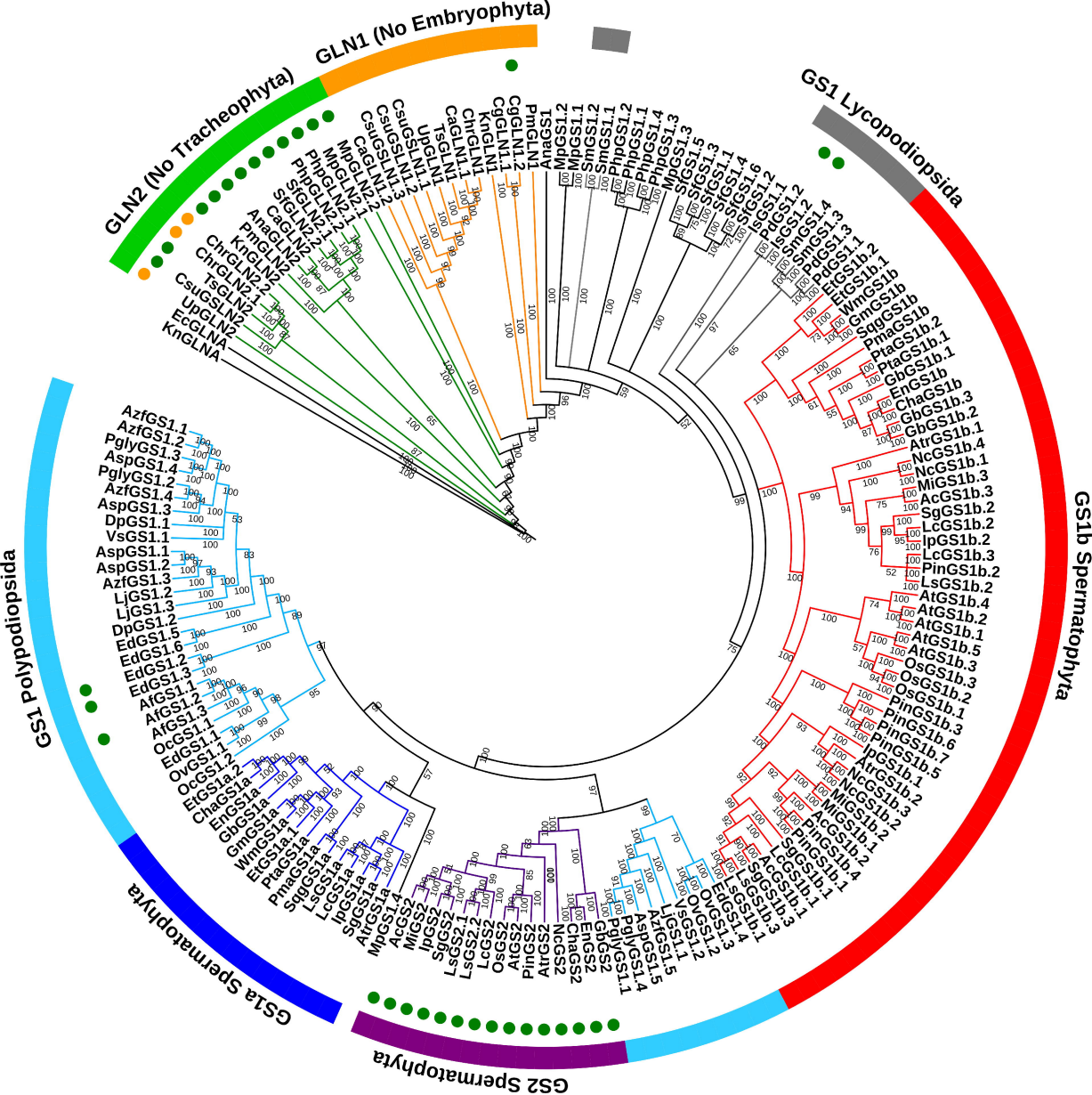


**Figure 1.** Phylogenetic tree of plant GS nucleotide sequences obtained following a Bayesian analysis. The first two letters of the sequence names correspond to genera and species listed in Table S1. Green circles highlight the sequences exhibiting a predicted plastidic localization. Orange circles highlight the sequences exhibiting a predicted mitochondrial localization. Branch lengths are not presented.

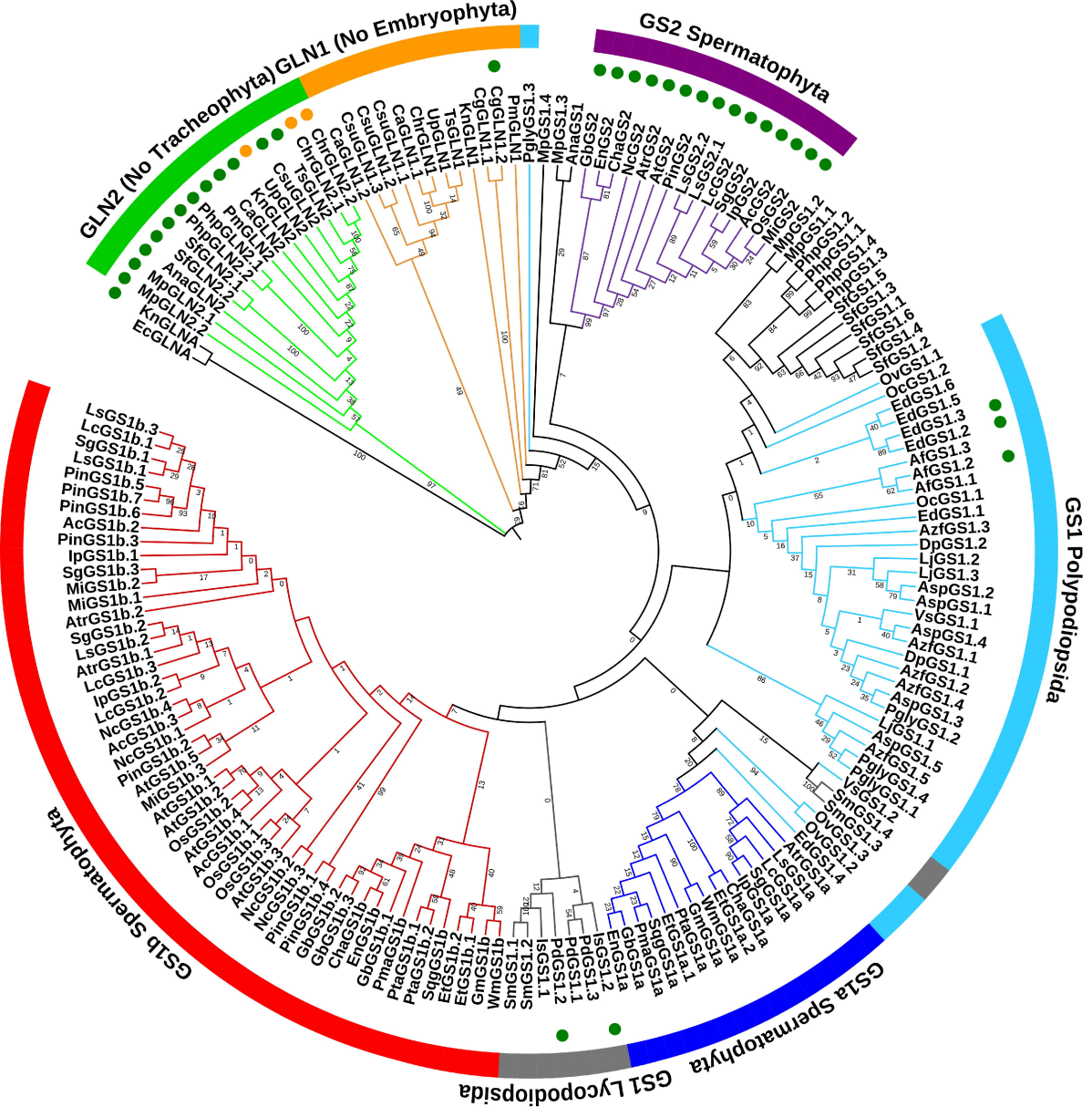


**Figure 2.** Protein phylogenetic tree of plant GS protein sequences following a Maximum Likelihood analysis. The first two letters of the sequence names correspond to genera and species listed in Table S1. Green circles highlight the sequences with a predicted chloroplastic localization. Orange circles highlight the sequences with a predicted mitochondrial localization. Branch lengths are not presented.

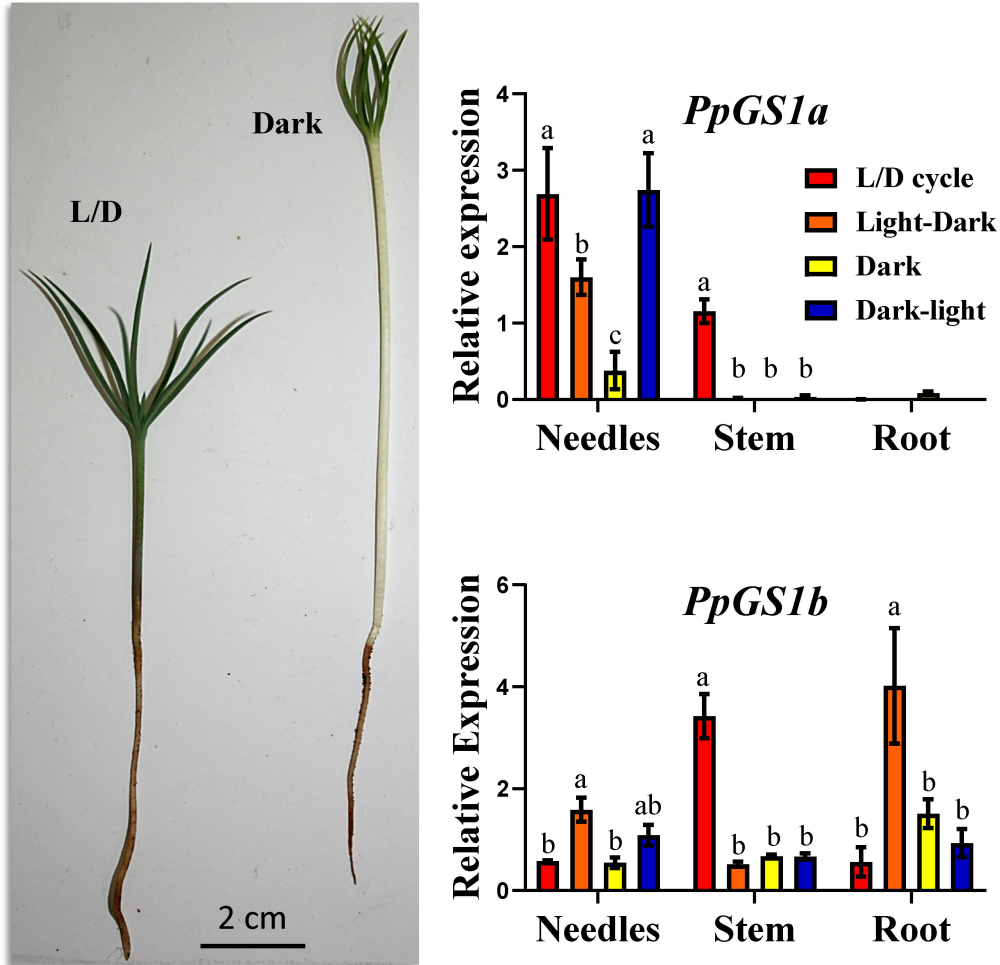


**Figure 3.** *PpGS1a* and *PpGS1b* gene expression in *Pinus pinaster* seedlings grown under different light regimes. L/D cycle (16h light /8h dark photoperiod, red bars), light photoperiod to continuous darkness transition (orange bars), continuous darkness (yellow bars) and complete darkness to light photoperiod transition (blue bars). Significant differences were determined using Two-way ANOVA that compare the mean for each condition with the mean of the other condition in the same organ. Letters above the columns indicate significant differences when a Tukey's post-hoc test ( $p < 0.05$ ) was applied.

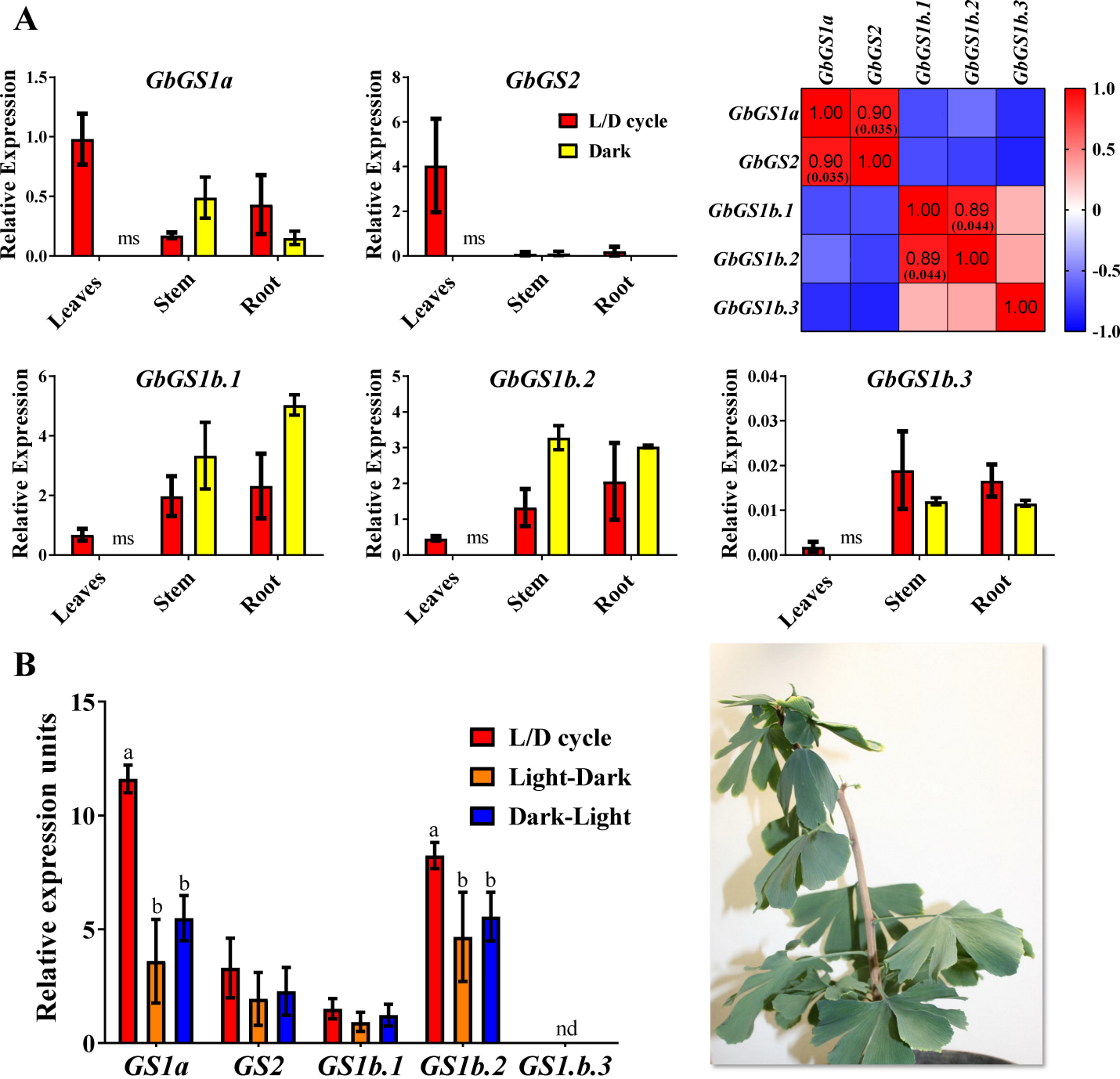


**Figure 4.** GS gene expression in *Ginkgo biloba* seedlings grown under different light regimes. Panel A. One-month old seedlings under L/D cycle: 16h light /8h dark photoperiod (red bars) and continuous darkness (yellow bars). A Pearson correlation test was applied to the expression level of the different GS genes to quantify their relationship indicated in the red squares. The significant  $p$ -values ( $< 0.05$ ) for the Pearson coefficient are indicated in brackets. Panel B. One-year old seedlings under L/D cycle (16h light /8h dark photoperiod, red bars), light photoperiod to continuous darkness transition (orange bars) and complete darkness to light photoperiod transition (blue bars). Significant differences were determined using a two-way ANOVA to compare the mean for each growth condition with the mean of the other conditions in the same organ. Letters above the columns indicate significant differences based on a Tukey's post-hoc test ( $p < 0.05$ ). nd= non-detected; ms= missing sample.

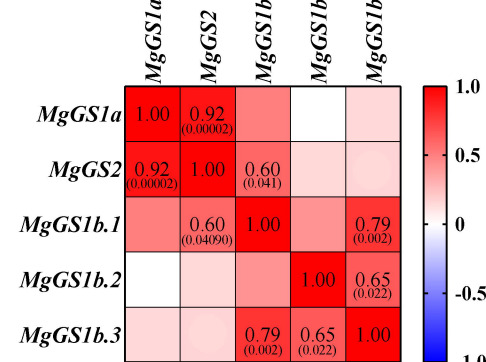
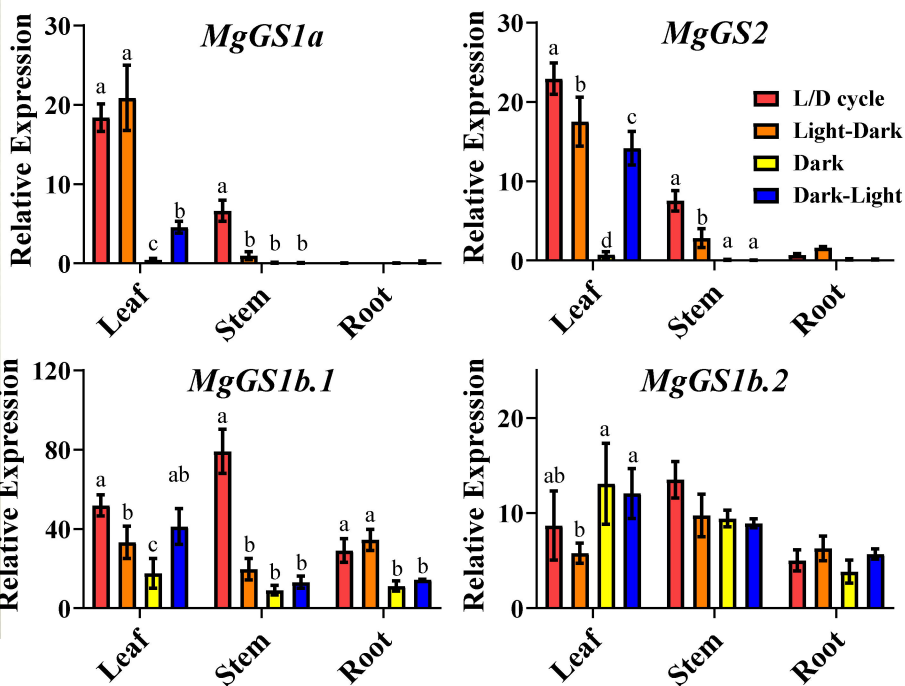


**Figure 5.** GS gene expression in *Magnolia grandiflora* seedlings grown under different light regimes. L/D cycle (16h light /8h dark photoperiod, red bars), light photoperiod to continuous darkness transition (orange bars), continuous darkness (yellow bars) and complete darkness to light photoperiod transition (blue bars). Significant differences were determined using Two-way ANOVA that compare the mean for each condition with the mean of the other condition for the same organ. Letters above the columns indicate significant differences when a Tukey's post-hoc test ( $p < 0.05$ ) was applied. Correlations between the expression levels of the different genes expressed in *M. grandiflora* using a Pearson Correlation test. The significant  $p$ -value ( $< 0.05$ ) are indicated in brackets.

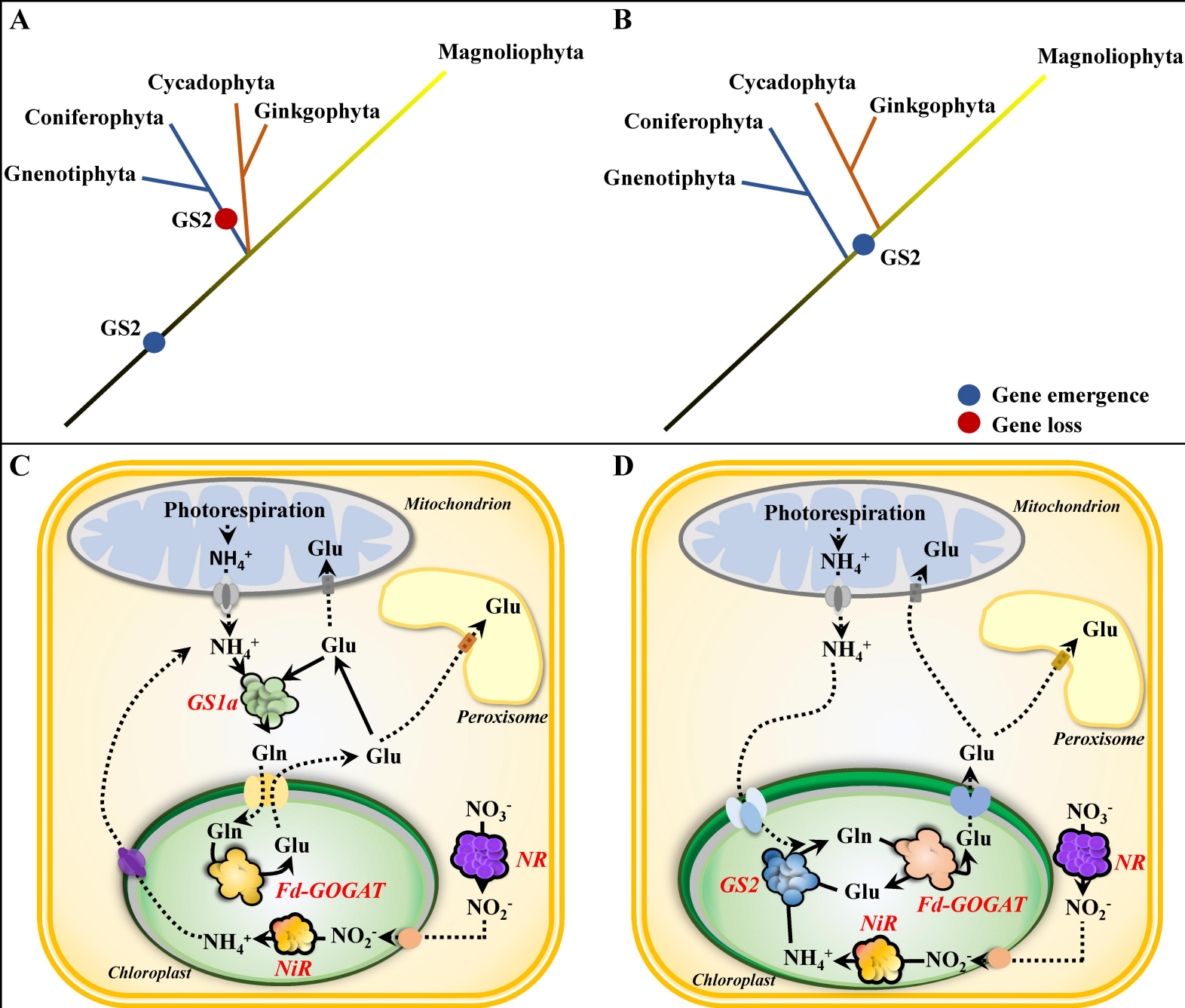


**Figure 6.** Schematic representation of GS2 emergence hypotheses. **A.** Two-event hypothesis. **B.** Single-event hypothesis. **C.** Simplified metabolic pathways in a photosynthetic cell in which ammonium assimilation is catalyzed by GS1a. **D.** Metabolic pathway of a photosynthetic cell in which ammonium assimilation is catalyzed by GS2. GS, glutamine synthetase. Fd-GOGAT, ferredoxin dependent glutamate synthase. NR, nitrate reductase. NiR, nitrite reductase.